

Force-dependent unfolding dynamics of spectrin R16:Resolving experimental contradiction and unveiling model consistency

Wanxing Zhang(张万星), Zhuwei Zhang(张珠伟), Zhenyong Xue(薛振勇), Yuhang Zhang(张宇航), Shimin Le(乐世敏), and Hu Chen(陈虎)

Citation: Chin. Phys. B, 2025, 34 (**8**): 088708. DOI: 10.1088/1674-1056/adbdbf
http://cpb.iphy.ac.cn; http://iopscience.iop.org/cpb

What follows is a list of articles you may be interested in

Combination of density-clustering and supervised classification for event identification in single-molecule force spectroscopy data

Yongyi Yuan(袁泳怡), Jialun Liang(梁嘉伦), Chuang Tan(谭创), Xueying Yang(杨雪滢), Dongni Yang(杨东尼), and Jie Ma(马杰)
Chin. Phys. B, 2023, 32 (**10**): 108702. DOI: 10.1088/1674-1056/acf03e

Coarse-grained simulations on interactions between spectrins and phase-separated lipid bilayers

Xuegui Lin(林雪桂), Xiaojie Chen(陈晓洁), and Qing Liang(梁清)
Chin. Phys. B, 2021, 30 (**6**): 068701. DOI: 10.1088/1674-1056/abf129

Interaction between human telomeric G-quadruplexes characterized by single molecule magnetic tweezers

Yi-Zhou Wang(王一舟), Xi-Miao Hou(侯锡苗), Hai-Peng Ju(车海鹏), Xue Xiao(肖雪), Xu-Guang Xi(奚绪光), Shuo-Xing Dou(窦硕星), Peng-Ye Wang(王鹏业), Wei Li(李伟)
Chin. Phys. B, 2018, 27 (**6**): 068701. DOI: 10.1088/1674-1056/27/6/068701

Improved data analysis method of single-molecule experiments based on probability optimization

Weili Zhai(翟伟利), Guohua Yuan(袁国华), Chao Liu(刘超), Hu Chen(陈虎)
Chin. Phys. B, 2018, 27 (**1**): 018703. DOI: 10.1088/1674-1056/27/1/018703

Catch-bond behavior of DNA condensate under tension

Li Wei (李伟), Wong Wei-Juan, Lim Ci-Ji, Ju Hai-Peng (车海鹏), Li Ming (李明), Yan Jie (严洁), Wang Peng-Ye (王鹏业)
Chin. Phys. B, 2015, 24 (**12**): 128704. DOI: 10.1088/1674-1056/24/12/128704

SPECIAL TOPIC — A celebration of the 90th Anniversary of the Birth of Bolin Hao

Force-dependent unfolding dynamics of spectrin R16: Resolving experimental contradiction and unveiling model consistency

Wanxing Zhang(张万星)[1], Zhuwei Zhang(张珠伟)[1,2], Zhenyong Xue(薛振勇)[1,2], Yuhang Zhang(张宇航)[1,2], Shimin Le(乐世敏)[1,†], and Hu Chen(陈虎)[1,2,‡]

[1] *Research Institute for Biomimetics and Soft Matter, Fujian Provincial Key Laboratory for Soft Functional Materials Research, Department of Physics, Xiamen University, Xiamen* 361005, *China*

[2] *Center of Biomedical Physics, Wenzhou Institute, University of Chinese Academy of Sciences, Wenzhou* 325000, *China*

(Received 28 December 2024; revised manuscript received 6 February 2025; accepted manuscript online 7 March 2025)

Spectrin domains, characterized by a distinctive triple helix structure, are crucial in physiological processes, particularly in maintaining membrane shape and crosslinking cytoskeletons. Previous research on the 16th domain of α-spectrin repeats (R16) has yielded conflicting results: bulk experiments showed an unfolding rate approximately two orders of magnitude faster than the zero-force result extrapolated from single-molecule force spectroscopy experiments using atomic force microscopy (AFM). To address this discrepancy, we investigated the folding and unfolding rates of R16 across a broader range of forces using magnetic tweezers (MT). Our findings reveal that AFM results at higher forces cannot be directly extrapolated to the low-force regime due to a nonlinear relationship between force and the logarithm of the unfolding rate. We demonstrated that two-dimensional model, structural-elastic model, and two-pathway model can all effectively explain the experimental data when they capture the core physics of the short unfolding distance at low forces. Our study provides a more comprehensive understanding of the unfolding dynamics of the spectrin domain, resolves previous contradictory experimental results, and highlights the common basis of different theoretical models.

Keywords: spectrin, protein folding and unfolding, force spectroscopy, magnetic tweezers

PACS: 82.37.Rs, 87.14.E–, 87.15.hm, 87.80.Nj

DOI: 10.1088/1674-1056/adbdbf **CSTR:** 32038.14.CPB.adbdbf

1. Introduction

Proteins are essential drivers of cellular processes, and the dynamics of their folding and unfolding have confounded scientists for more than fifty years.[1] Understanding the dynamics of the conformation transition is crucial for both biological processes and the development of novel biomaterials.[2] In single-molecule manipulation experiments, force is often used as a controllable variable to probe protein conformational transitions.[3] Bell's model[4] is widely used to describe the unfolding dynamics of proteins, which shows a linear relationship between the logarithm of unfolding rate and force. However, recent investigations of the dynamic features of numerous proteins have revealed anomalies in the protein unfolding transition dynamics measured in a wider force range. In some cases, the slope of the logarithm of unfolding rate increases with increasing force, as seen in I27[5] and src SH3,[6] while the unfolding rates of some other proteins show the opposite force-dependence, such as GB1[7] and CSP.[8] These anomalous scenarios have led to the proposal of novel models aiming to explain these phenomena, such as two-dimensional (2D) model,[9] structural-elastic model,[10] and multi-pathway model.[11]

Spectrin is a chain-like protein composed of multiple repeating triple-helical modules, forming a flexible and resilient structure.[12] It has been recognized as a force-bearing protein involved in various cellular activities. Spectrin plays a pivotal role in the axon growth process through interacting with actin fiber.[13–15] Additionally, spectrin is crucial in endothelial cells during the process of sensing shear forces.[16,17] Given the force-dependent physiological roles of spectrin and its distinctive triple-helical structure, it is important to investigate the mechanical properties of this protein.

The biochemical properties of the sixteenth domain of α-spectrin repeat (R16) have been investigated through bulk experiments[18,19] and the mechanical properties have been investigated through atomic force microscopy (AFM) stretching experiments.[20,21] The unfolding rate at zero concentration of denaturant $k_u^0 = 2.6 \times 10^{-3}$ s^{-1}[22] extrapolated from bulk experiments is two orders of magnitude faster than that obtained from AFM stretching experiments 3.3×10^{-5} s^{-1}.[20] The force and urea are employed to induce the protein unfolding from different reaction coordinates. The extrapolated unfolding rates at zero force and zero concentration of denaturant should be the same if both linear extrapolations are valid. Subsequently, this large discrepancy might arise from two possible

†Corresponding author. E-mail: leshimin@xmu.edu.cn

‡Corresponding author. E-mail: chenhu@xmu.edu.cn

© 2025 Chinese Physical Society and IOP Publishing Ltd. All rights, including for text and data mining, AI training, and similar technologies, are reserved.

reasons. First, extrapolating unfolding rates from high urea concentrations ($\geq$ 2.5 M) to zero concentration may not be valid. Second, the extrapolation of AFM force-dependent unfolding rates to zero-force conditions may not be valid. AFM stretching experiments[21] can monitor the dynamic behavior of single molecules with high time and spatial resolution. The unfolding force range of spectrin in AFM experiments is 25–35 pN with loading rate from 1000 pN/s to 10000 pN/s, but it is hard to measure unfolding rate at forces smaller than 10 pN by AFM.

The force range and loading rate applied to spectrin protein in cells have not been measured directly. Based on studies of cell–substrate interactions, the loading rates of integrin-based adhesion are from 0.5 pN/s to 2.0 pN/s, and the force is from several pN to tens of pN.[23] In this study, we used magnetic tweezers (MT)[7,24] to directly measure the folding and unfolding rates at similar loading rate and force range, aiming to test whether the extrapolation of AFM results to zero force is valid. We found that the logarithm of the unfolding rates at forces lower than 15 pN starts to show nonlinear force dependence and zero-force unfolding rate is in the order of 10^{-3} s^{-1} which is close to the bulk experiment. Therefore, the linear extrapolation of AFM results will yield a large deviation at zero force. Furthermore, we found that two-pathway model, 2D model, and structural-elastic model can all explain the experimental data very well, if they assume a zero-force unfolding rate similar to the bulk biochemical experiment and a short unfolding distance at low forces.

2. Materials and methods

2.1. Protein expression and purification

Recombinant protein constructs (Histag-Avitag-FH1-R16-FH1-Spytag) were created by inserting gene sequences of R16 into the pET151 vector by GenScript Biotech. Biotinylated proteins were expressed in *E. coli* strain BL21 (DE3) co-transferred together with pBirA plasmid. Protein expression was induced with IPTG, and proteins were purified using Ni-NTA resin and Superdex 200 column chromatography. Then the proteins were aliquoted, flash-frozen in liquid nitrogen, and stored at −80 °C.

2.2. Sample preparation and magnetic tweezers measurement

Cleaned coverslips were functionalized with APTES and used to build flow chambers which were treated with Sulfo-SMCC to link Spycatcher proteins with Cysteine at N-terminus. Then R16 protein constructs and streptavidin-coated paramagnetic beads were flowed into the chamber sequentially to form protein tethers. Figure 1(a) displays the schematic figure of MT measurement. Protein of R16 domain was stretched by magnetic tweezers with the protein construct Histag-Avitag-FH1-R16-FH1-Spytag. Biotin ligated to Avitag was used to bind the streptavidin-coated paramagnetic bead, and Spytag was used to form covalent bond with Spycatcher on the glass surface. Magnetic tweezers were built based on an inverted microscope. It can control the stretching force by moving the permanent magnets above the flow chamber. The reference polystyrene bead stuck on the coverslip surface was used to eliminate the mechanical drift during the measurement. The height of the paramagnetic bead was recorded with nanometer resolution, which reflects the conformation transition of the tethered protein. The sampling rate of the magnetic tweezers was 200 Hz. More details of the experimental procedures can be found in our previous work.[8]

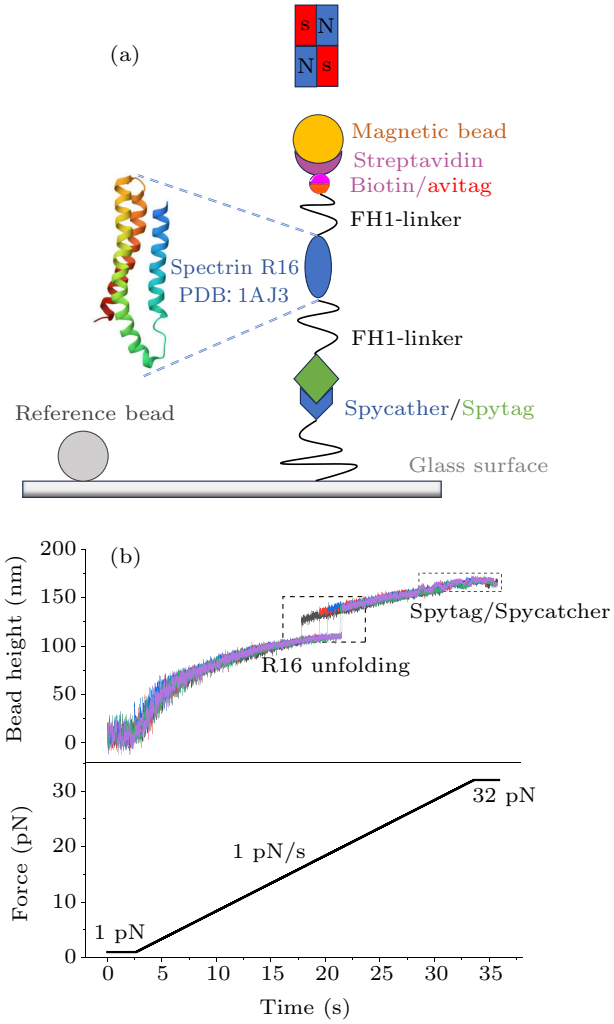


Fig. 1. (a) Experimental schematic of stretching the protein construct Avitag(biotin)-FH1-R16-FH1-Spytag by MT. (b) The raw data of multiple cycles of stretching with a loading rate of 1 pN/s. R16 unfolding events are observed with abrupt jump of bead height. The zipping and unzipping events occurring at about 30 pN are the fingerprints of SpyCatcher/Spytag complex.

3. Results

3.1. Force-ramp experiment

Figure 1(b) shows several curves of bead height measured by force-ramp experiments. At the beginning, R16 is

in its native state with stretching force of 1 pN. Then force is increased to 32 pN with a constant loading rate of 1 pN/s. During this force-increasing process, the unfolding signal of R16 and the equilibrium unzipping/zipping signal of the Spycatcher/Spytag complex can be observed. The signal from the Spycatcher/Spytag at about 30 pN is a fingerprint to indicate the correct single-protein tether.[25]

Theoretically, the force-dependent unfolding rate can be obtained from the distribution of unfolding forces if enough data are collected.[26,27] But it is only in the force range with non-zero distribution, and the experimental error is related to the number of counts in the bins of statistical histogram.

3.2. Force-jump experiment

To address the significant discrepancy in zero-force unfolding rates between bulk experiments and AFM stretching experiments, we aim to obtain the unfolding rates in the low-force regime. Subsequently, we employed the force-jump experiment to obtain transition rates over large force range. Both force-dependent folding and unfolding transitions can be studied by force-jump experiment.

During the unfolding process, we first applied a small stretching force of 1 pN for 10 s to ensure the protein folds to the native state, then increased the force to a specific value until the unfolding occurs. Afterward, we reduced the force to 1 pN for 10 s to let the protein fold to its native state. Multiple cycles can be done to collect enough data for analysis. Figure 2(a) exhibits the unfolding processes at 17.5 pN. During the folding process, we initially applied 24 pN to unfold the protein, then reduced the force to a lower value to wait for the folding event. Figure 2(b) shows the folding processes at 5 pN.

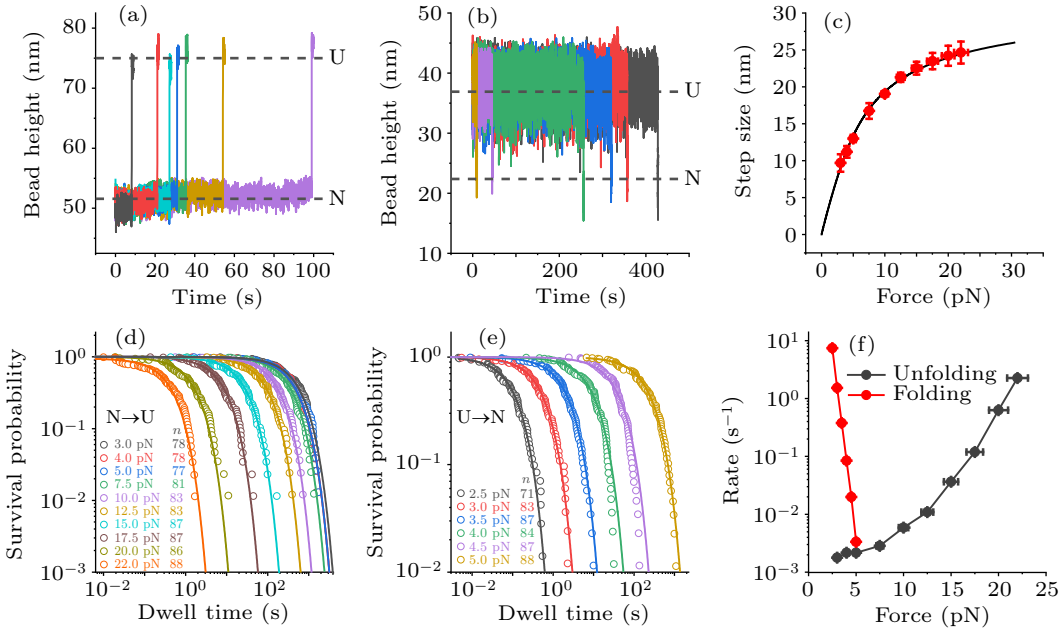


Fig. 2. Folding and unfolding rates obtained from the force-jump experiment. (a) The raw data of unfolding process at 17.5 pN. (b) Folding process at 5 pN. (c) The unfolding step size as a function of force agrees with the theoretical curve. (d) The survival probabilities of the native state at 3–22 pN are fitted with single-exponential curves to get the unfolding rates. (e) The survival probabilities of unfolded state at 2.5–5 pN are fitted with single-exponential curves to get the folding rates. The numbers of data points are given in the legend. (f) The mean folding and unfolding rates from three independent protein tethers. The error bars of rate are smaller than the symbol and the force uncertainty is estimated to be 5%.

The force-dependent step sizes are shown in Fig. 2(c). The extension of the unfolded peptide along the force direction, x_{chain}, can be modeled by a worm-like chain (WLC)

$$\frac{FA}{k_{\text{B}}T} = \frac{x_{\text{chain}}}{L} + \frac{1}{4}\left(1 - \frac{x_{\text{chain}}}{L}\right)^{-2} - \frac{1}{4}, \tag{1}$$

where F denotes the applied force, A is the persistence length of the protein, k_{B} represents the Boltzmann constant, T is the absolute temperature, L means the contour length of the protein, calculated by $L = Nb = 38.2$ nm, and N means the number of the amino acids and b is the average length of each amino acid set to 0.39 nm from fitting the relationship between the force and step size. At low forces, the deformation of the folded native state can be ignored, and only the orientation fluctuation will affect its extension. Therefore, the native structure of the protein can be modeled as a rigid body and its force-dependent extension follows

$$x_{\text{N}}(F) = l_{\text{N}} \coth\left(\frac{F l_{\text{N}}}{k_{\text{B}}T}\right) - \frac{k_{\text{B}}T}{F}, \tag{2}$$

where l_{N} represents the N–C distance of the native state of the protein. Thereby, Fig. 2(c) presents the force-dependent step size $\Delta x(F) = x_{\text{chain}} - x_{\text{N}}$ which agrees with the theoretical result.

Besides the step size results, we also collected dwell times of the folded or unfolded states at different constant

forces, and fitted the survival probabilities of the native state (Fig. 2(d)) and the unfolded state (Fig. 2(e)) using single-exponential functions to obtain unfolding rates and folding rates, respectively. Figure 2(f) shows the force-dependent folding rates obtained from 2.5 pN to 5 pN and unfolding rates from 3 pN to 22 pN. All data were collected from three independent protein tethers. The logarithm of the folding rate is almost a linear function of force. On the other hand, the logarithm of the unfolding rate shows non-linear force dependence, with the slope decreasing with decreasing force.

3.3. Equilibrium constant force experiment

The critical force, at which folding rate is equal to unfolding rate, is ~ 5 pN. When stretching force is maintained at constant value close to the critical force, both folding and unfolding transition can be recorded. The left panel of Fig. 3(a) presents the time course of bead height at forces of 4.0 pN, 4.5 pN, and 5.0 pN, and the right panel is the relative frequency of bead height obtained from the histogram of the smoothed data. The relative frequency can be fitted by a two-peak Gaussian function with each peak corresponding to folded or unfolded state. The probability of the unfolded state increases with increasing force.

Figure 3(b) illustrates the single exponential fitting of the survival probabilities of the unfolded state and native state to obtain the folding and unfolding rates shown in Fig. 3(c), which are consistent with the results obtained from the force-jump experiment. From the critical force $F_c = 4.8$ pN based on the equilibrium constant force experiment and the force-dependent step size (Fig. 2(c)), the folding free energy ΔG_0 can be determined by $\Delta G_0 = \int_0^{F_c} \Delta x(f)\,\mathrm{d}f = 8.2\ k_B T$.

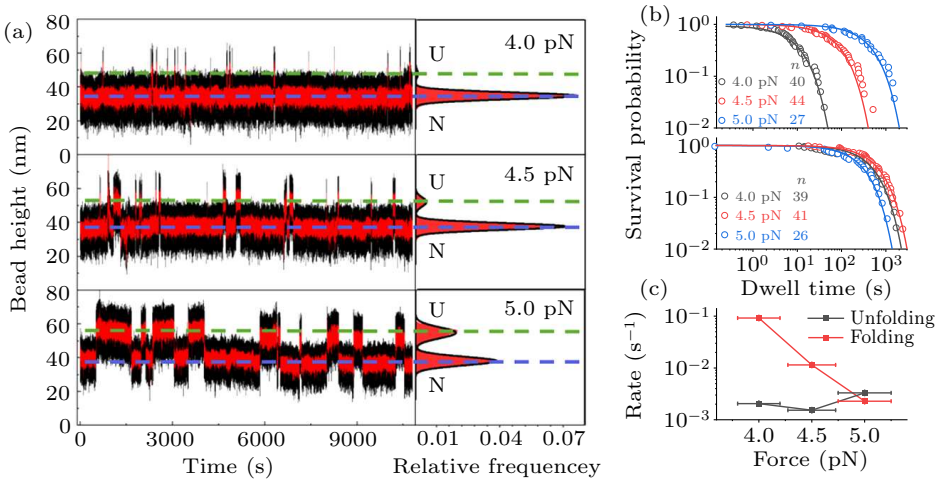


Fig. 3. Folding and unfolding rates obtained from the equilibrium constant force experiment. (a) The raw data (black) are recorded for 10000 s at 4 pN, 4.5 pN, 5 pN and smoothed by a 0.1-s time window (red). The right panel shows the relative frequencies of smoothed data which are fitted by two-peak Gaussian functions. (b) The survival probabilities of unfolded state (top panel) and native state (lower panel) at 4–5 pN. Single-exponential fittings give the folding and unfolding rates. (c) The force-dependent folding and unfolding rates obtained from the equilibrium measurement. The force is estimated to have 5% uncertainty.

3.4. Analysis of nonlinear unfolding dynamics

Besides the R16 domain of α-spectrin, the nonlinear force-dependent unfolding rate has also been observed in the β-spectrin 12th–15th domains.[28] Therefore, similar super-exponential unfolding rate might be prevalent in the spectrin super family, which deserves a systematic modeling study to understand this phenomenon.

The energy landscape is an important tool for understanding dynamic properties of proteins. In single-molecule force spectroscopy experiment, the molecule extension x along the stretching force direction is usually used as a reaction coordinate to depict the free energy landscape $G(x)$.[29,30] Whereas, this one-dimensional free energy landscape is insufficient to describe the dynamic behavior of biomolecules especially when the energy landscape is frustrated. There is a criterion[31] to determine whether a one-dimensional free energy landscape is enough to give force-dependent unfolding rate $k_u(F)$. If $k_u(F)$ satisfies both of the following conditions:

$$\frac{\mathrm{d}}{\mathrm{d}F}\log k_u(F) \geq 0, \quad \frac{\mathrm{d}^2}{\mathrm{d}F^2}\log k_u(F) \leq 0, \tag{3}$$

the underlying free energy landscape could be described in one-dimensional space, otherwise it must be multidimensional.

As for the case of R16, the unfolding rate scenario fails to satisfy the latter of Eq. (3), so the underlying free energy landscape of R16 should be multidimensional. There are several methods to address the complexities of the multidimensional landscape dynamics, like 2D model,[9] structural-elastic model,[10] and two-pathway model.[11,32] Subsequently, we employ the empirical formula to build the relationship between the zero-force unfolding rate k_u^0 and activation energy barrier $\Delta G^{\ddagger}$ in all three models: $k_u^0 = k^* \exp\left(-\beta \Delta G^{\ddagger}\right)$, where $k^* = 10^6\ \mathrm{s}^{-1}$ is the empirical intrinsic transition rate and $\beta = 1/(k_B T)$.

3.4.1. Two-dimensional model

The minimal multidimensional model is a 2D model which provides a general approach to depict the protein unfolding dynamics by incorporating the influence of a slow coordinate Q:[27]

$$G(x,Q) = G_0(Q) + \frac{1}{2}k(Q)[x - x_0(Q)]^2 - Fx, \tag{4}$$

where $G_0(Q)$ denotes the free energy at zero force, $k(Q)$ is the molecule's spring constant along the extension direction, and $x_0(Q)$ is the most probable value of the extension at a given Q and zero force. When Q is the reaction coordinate with the slowest dynamics, the 2D model in Eq. (4) generates a conformation transition dynamics which can be described by a diffusion process crossing the free energy barrier. Thereby, the relationship between applied force and unfolding rate is given by[9,33]

$$k_u(F) = k^* \Delta q(F)\, e^{-\beta \Delta G^{\ddagger} \Delta q^3(F)}, \tag{5}$$

with $\Delta q(F) = \Delta Q^{\ddagger}(F)/\Delta Q_0^{\ddagger}$, where $\Delta Q^{\ddagger}(F)$ represents the distance between the folded state and the transition state along the reaction coordinate Q and $\Delta Q_0^{\ddagger} = \Delta Q^{\ddagger}(0)$.

Our experimental data show that the slope of the logarithm of force-dependent unfolding rates tends to zero when the force decreases, which indicates that the unfolding distance at zero force along extension can be set as zero. Therefore, the expression for $\Delta q(F)$ can be simplified as[9]

$$\Delta q^2(F) = 1 - \frac{\Delta k^{\ddagger}/(3\Delta G^{\ddagger} k_{\cup}^{02})}{1 - \Delta k^{\ddagger}/k_{\cup}^0} F^2 \tag{6}$$

$$= 1 - \frac{F^2}{k \Delta G^{\ddagger}}, \tag{7}$$

where $k_{\cup}^0$ is the stiffness of the folded molecule in the absence of force, $\Delta k^{\ddagger} = k_{\cup}^0 - k_{\cap}^0$ represents the difference between $k_{\cup}^0$ and the stiffness of the transition state $k_{\cap}^0$, $k = 3k_{\cup}^{02}(1 - \Delta k^{\ddagger}/k_{\cup}^0)/\Delta k^{\ddagger}$ is a parameter derived from $k_{\cup}^0$ and $k_{\cap}^0$.

Consequently, the fitting of experimental data with Eq. (5) yields two parameters $\Delta G^{\ddagger} = 20.5 \pm 0.1\ k_B T$ and $k = 22.4 \pm 0.7$ pN/nm. As $k_u(F)$ depends only on $\Delta q(F)$ which is the normalized value of $\Delta Q^{\ddagger}(F)$, the exact value of $\Delta Q_0^{\ddagger}$ cannot be determined.

3.4.2. Structural-elastic model

Another physical model, based on the structural-elastic properties of the native state and transition state, was proposed to illustrate the abnormal unfolding scenario.[5,10] The original model assumes that the transition state has a well-defined structure with a folded core and a flexible peptide, and $k_u(F)$ follows the equation

$$k_u(F) = k^* \exp\left[-\beta\left(\Delta G^{\ddagger} + \eta F^{\frac{1}{2}} - \sigma F - \frac{\alpha F^2}{2}\right)\right], \tag{8}$$

where η, σ, and α are parameters determined by the extensions and elasticities of the native state and transition state. $\eta = L^* \sqrt{k_B T/A}$, where L^* denotes the contour length of the flexible peptide. $\sigma \sim L^* + (b^* - b^0)$ with b^0 and b^* as the lengths of native state and transition state, respectively. $\alpha = b^*/\gamma^* - b^0/\gamma^0$, where γ^* and γ^0 are the stretching modulus of native state and transition state, respectively.

Here we suppose that the same equation applies to other proteins as long as the elastic deformations of native state and transition state play an important role in the unfolding process. The fitting of $k_u(F)$ of spectrin R16 domain gives $\alpha = 0.17 \pm 0.03$ nm/pN, $\Delta G^{\ddagger} = 20 \pm 1\ k_B T$, and η and σ around zero with large relative uncertainty. Therefore, we set zero values for η and σ and obtained a fitting curve which agrees with experimental data very well with $\alpha = 0.123 \pm 0.003$ nm/pN and $\Delta G^{\ddagger} = 20.4 \pm 0.1\ k_B T$. The result is consistent with the hypothesis of zero unfolding distance at zero force in the 2D model.

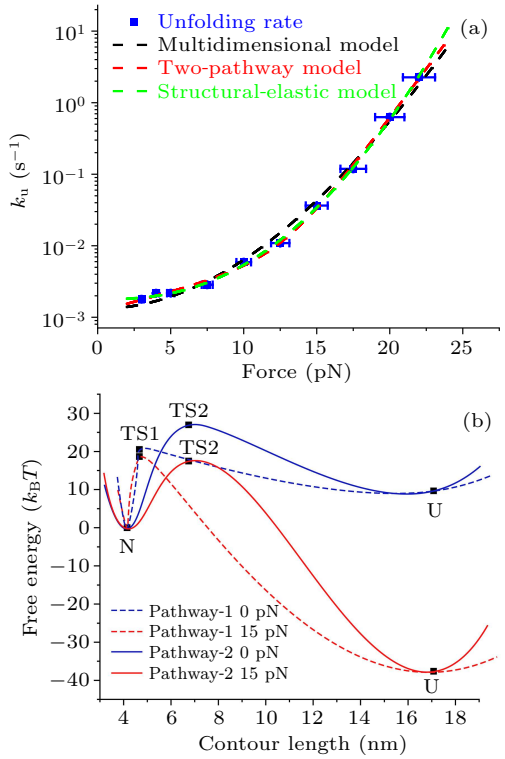


Fig. 4. (a) The force-dependent unfolding rates are fitting with 2D model, two-pathway model, and the structural-elastic model. (b) The free energy landscape of pathway-1 and pathway-2 in two-pathway model at zero force and 15 pN.

3.4.3. Two-pathway model

Affected by the roughness of the 2D free energy landscape,[34] the protein may unfold through more than one pathway. The two-pathway model was used to explain the unfolding dynamics of src SH3 protein.[6,35] The unfolding dynamics of R16 can be modeled by a similar two-pathway model which gives unfolding rate as summation of the unfolding rate of each pathway

$$k_u(F) = k_L^0 e^{\beta F x_L} + k_H^0 e^{\beta F x_H} \tag{9}$$

$$= k^{*}\left[\mathrm{e}^{-\beta(G_{\mathrm{L}}^{\ddagger}-Fx_{\mathrm{L}})}+\mathrm{e}^{-\beta(G_{\mathrm{H}}^{\ddagger}-Fx_{\mathrm{H}})}\right], \quad (10)$$

where k_{L}^{0} and k_{H}^{0} are extrapolated zero-force unfolding rates, x_{L} and x_{H} are unfolding distances, $\Delta G_{\mathrm{L}}^{\ddagger}$ and $\Delta G_{\mathrm{H}}^{\ddagger}$ are zero-force unfolding barriers of the pathways which dominate at low force and high force, respectively.

Fitting of experimental data with this two-pathway model Eqs. (9) and (10) gives $k_{\mathrm{L}}^{0}=(1.2\pm0.4)\times10^{-3}$ s^{-1}, $k_{\mathrm{H}}^{0}=(2\pm2)\times10^{-6}$ s^{-1}, $x_{\mathrm{L}}=0.5\pm0.1$ nm, $x_{\mathrm{H}}=2.6\pm0.1$ nm, $\Delta G_{\mathrm{L}}^{\ddagger}=20.5\pm0.1\ k_{\mathrm{B}}T$ and $\Delta G_{\mathrm{H}}^{\ddagger}=27.0\pm0.5\ k_{\mathrm{B}}T$. Notably, the k_{L}^{0} is about three orders of magnitude faster than k_{H}^{0}, and is consistent with the previous bulk experimental result $\sim3\times10^{-3}$ s^{-1}.[22] The unfolding distance x_{L} is only one fifth of x_{H}. Based on these fitting results, we construct the free energy landscape in Fig. 4(b). We designate the dominant pathway in the low force regime as pathway-1 and the other pathway as pathway-2.

4. Discussion and conclusion

In summary, we measured the folding and unfolding rates of R16 domain with MT. Our findings reveal an unusual characteristic in spectrin's unfolding dynamics: it is relatively insensitive to force in the low-force regime (<15 pN) but becomes more force-sensitive in the high-force regime (>15 pN). This characteristic indicates that spectrin can sustain tension within a threshold and respond to tension above this threshold, thus playing an essential role as an endothelial mechanosensor.[17]

To explain the non-linear force-dependent unfolding rate, three models which have been proposed previously in studies of different proteins are used to fit our data. The fitting results, as shown in Fig. 4(a), demonstrate that all fitting curves closely align with the experimental data. In our study, the analysis uses an empirical formula to establish the relationship between zero-force unfolding rate and activation energy barrier, facilitating a clearer comparison between these models. The three models yield similar values of the activation energy barrier, consistent with the previous bulk experiment.[22] Our results indicate that the linear extrapolation of unfolding rate measured in bulk experiment to zero concentration of denaturant is valid in the case of spectrin R16.

We explain the unfolding scenario within the multidimensional energy landscape framework intrigued by the criterion Eq. (3). In these models, the extension of molecule x alone is insufficient to depict the protein dynamics. For the 2D model, an additional slow reaction coordinate Q orthogonal to the molecule extension x is introduced to capture the multidimensional unfolding characteristics. The structural-elastic model considers that the native state and the transition state have the same zero-force extension but different stretching moduli. Therefore, both the extension of the native state and the transition state are force-dependent variables, and their difference determines the force-dependent barrier height. With a given extension, whether the conformation belongs to native state or transition state is not determined. Therefore, the structural-elastic model is intrinsically not a one-dimensional model, though only extension x appears in the model. In the two-pathway model, the pathway index (1 and 2) serves as a second parameter in addition to the extension x to describe the pathway-switching phenomenon. Therefore, the two-pathway model is also a 2D model.[36]

Though all three models are intrinsically multidimensional, the two-pathway model postulates two pathways with two distinct transition states. The other two models assume only one pathway with one single transition state whose extension might change with force. The reason why all three models explain the experimental data of R16 domain very well must be that they all grasp the same essential property of the transition dynamics. Comparing the hypothesis and fitting parameters of each model, the essential properties should be that the transition state has an extension very close to the native state at small force. With increasing force, the transition state becomes longer or the pathway switches to the one with a longer transition state. From our perspective, the 2D model is an abstract one that does not define the slow reaction coordinate specifically. In contrast, the other two models have strong assumptions regarding the properties of the transition states or transition pathways, which might be tested experimentally in the future.

In conclusion, this study employs three different models to explain the non-linear relationship between the logarithm of the unfolding rates of the α-spectrin R16 domain and the stretching force, offering new insights into the multidimensional energy landscape of protein dynamics. Our current experimental results are not enough to distinguish which model gives the true molecular mechanism of the unfolding dynamics of α-spectrin R16 domain. New techniques which can detect more dimensional signals are desired to reveal detailed mechanism of protein conformational transitions.

Acknowledgements

Project supported by the National Natural Science Foundation of China (Grant Nos. 12174322, 12474200, 32271367, and 12204389), 111 Project (B16029), and Research Grant from Wenzhou Institute.

References

[1] Dill K A and MacCallum J L 2012 *Science* **338** 1042
[2] Wu J, Li P, Dong C, Jiang H, Bin Xue, Gao X, Qin M, Wang W, Bin Chen and Cao Y 2018 *Nat. Commun.* **9** 620
[3] Neuman K C and Nagy A 2008 *Nat. Methods* **5** 491
[4] Bell G I 1978 *Science* **200** 618
[5] Yuan G, Le S, Yao M, Qian H, Zhou X, Yan J and Chen H 2017 *Angewandte Chemie International Edition* **56** 5490

[6] Jagannathan B, Elms P J, Bustamante C and Marqusee S 2012 *Proc. Natl. Acad. Sci. USA* **109** 17820

[7] Guo Z, Hong H, Yuan G, Qian H and Chen H 2020 *Phys. Rev. Lett.* **125** 198101

[8] Hong H, Guo Z, Sun H, Yu P, Su H, Ma X and Chen H 2021 *Communications Chemistry* **4** 156

[9] Suzuki Y and Dudko O K 2010 *Phys. Rev. Lett.* **104** 048101

[10] Guo S, Tang Q, Yao M, You H, Le S, Chen H and Yan J 2018 *Chem. Sci.* **9** 5871

[11] Pierse C A and Dudko O K 2017 *Phys. Rev. Lett.* **118** 088101

[12] Pascual J, Pfuhl M, Walther D, Saraste M and Nilges M 1997 *Journal of Molecular Biology* **273** 740

[13] Franze K 2020 *Annual Review of Cell and Developmental Biology* **36** 61

[14] Khan M I, Ferdous S F and Adnan A 2021 *Multiscale Science and Engineering* **3** 185

[15] Lorenzo D N, Edwards R J and Slavutsky A L 2023 *Nature Reviews Neuroscience* **24** 195

[16] Duan R, Kim J H, Shilagardi K, Schiffhauer E S, Lee D M, Son S, Li S, Thomas C, Luo T, Fletcher D A, Robinson D N and Chen E H 2018 *Nature Cell Biology* **20** 688

[17] Mylvaganam S, Plumb J, Yusuf B, Li R, Lu C Y, Robinson L A, Freeman S A and Grinstein S 2022 *Nature Cell Biology* **24** 1226

[18] Scott K A and Clarke J 2005 *Protein Science* **14** 1617

[19] Wensley B G, Kwa L G, Shammas S L, Rogers J M, Browning S, Yang Z and Clarke J 2012 *Proc. Natl. Acad. Sci. USA* **109** 17795

[20] Rief M, Pascual J, Saraste M and Gaub H E 1999 *Journal of Molecular Biology* **286** 553

[21] Randles L G, Rounsevell R W and Clarke J 2007 *Biophysical Journal* **92** 571

[22] Scott K A, Batey S, Hooton K A and Clarke J 2004 *Journal of Molecular Biology* **344** 195

[23] Hu Y, Li H, Zhang C, Feng J, Wang W, Chen W, Yu M, Liu X, Zhang X and Liu Z 2024 *Cell* **187** 3445

[24] Chen H, Fu H, Zhu X, Cong P, Nakamura F and Yan J 2011 *Biophys. J.* **100** 517

[25] Guo Z, Hong H, Sun H, Zhang X, Wu C X, Li B, Cao Y and Chen H 2021 *Nanoscale* **13** 11262

[26] Dudko O, Hummer G and Szabo A 2006 *Phys. Rev. Lett.* **96** 108101

[27] Dudko O K, Hummer G and Szabo A 2008 *Proc. Natl. Acad. Sci. USA* **105** 15755

[28] Renn J P, Bhattacharyya S, Bai H, He C, Li H, Oberhauser A F, Marko J F, Makarov D E and Matouschek A 2019 *Scientific Reports* **9** 11101

[29] Sun H, Guo Z, Hong H, Zhang Z, Zhang Y, Wang Y, Le S and Chen H 2023 *Phys. Rev. Lett.* **131** 218402

[30] Ma X, Sun H, Hong H, Guo Z, Su H and Chen H 2022 *Phys. Rev. E* **106** 024404

[31] Zhuravlev P I, Hinczewski M, Chakrabarti S, Marqusee S and Thirumalai D 2016 *Proc. Natl. Acad. Sci. USA* **113** E715

[32] Dudko O K 2009 *Proc. Natl. Acad. Sci. USA* **106** 8795

[33] Suzuki Y and Dudko O K 2011 *The Journal of Chemical Physics* **134** 065102

[34] Wensley B G, Batey S, Bone F A C, Chan Z M, Tumelty N R, Steward A, Kwa L G, Borgia A and Clarke J 2010 *Nature* **463** 685

[35] Guinn E J, Jagannathan B and Marqusee S 2015 *Nat. Commun.* **6** 6861

[36] Barkan C O and Bruinsma R F 2023 *Phys. Rev. Research* **5** 023161